COMMUNICATION

Late-stage ligand functionalization via the Staudinger reaction using phosphine-appended 2,2'-bipyridine†

Received 00th January 2020,
Accepted 00th January 2020

DOI: 10.1039/x0xx00000x

Deeb Taher,[a,b] Jessica R. Wilson,[a] Grayson Ritch,[a] Matthias Zeller,[c] Nathaniel K. Szymczak[a*]

The ability of a phosphine-appended-2,2'-bipyridine ligand ($(Ph_2P)_2bpy$) to serve as a platform for late-stage ligand modifications was evaluated using tetrahedral $(Ph_2P)_2bpyFeCl_2$. We employed a post-metalation Staudinger reaction to install a series of functionalized arenes, including those containing Brønsted and Lewis acidic groups. This reaction sequence represents a versatile strategy to both tune the ligand donor properties as well as directly incorporate appended functionality.

Access to ligand architectures featuring diverse steric and electronic properties is a key strategic approach that underpins most coordination chemistry and catalyst optimization. Although most commonly achieved through early-stage (pre-metalation) routes, diversification by late-stage functionalization offers a modular approach to build complexity from a single platform. Late-stage functionalization reactions can be used to introduce additional moieties into a ligand scaffold, altering the ability to direct reactivity by using a combination of primary as well as secondary coordination sphere interactions.[1] The most common strategies to modify a metal complex after metalation are through addition or subtraction of Brønsted or Lewis acids which, in some instances, provide ligand types that are not accessible using pre-metalation functionalization routes.[2]

The need for late-stage ligand modification is apparent for ligands containing appended Lewis acids. In such cases, ligand lone pairs can form quenched acid/base adducts often providing an inert adduct.[3] For borane-appended Lewis acids, a common strategy to overcome this challenge is via late stage hydroboration.[3a] However, implementing an alternative late stage functionalization strategy that is independent of Lewis acid would be complementary to existing protocols and enable access to a broader ligand chemical space.

One late-stage functionalization route is the assembly of iminophosphoranes ($R_3P{=}NR$) from the corresponding phosphine via the Staudinger reaction. These units are most commonly encountered as synthetic intermediates,[4,5] and are also competent ligands.[6,7] Generation of $R_3P{=}NR$ units from the corresponding R_3P affords ligands with desirable donor properties: $R_3P{=}NR$ ligands are strong σ-donor, weak π-acceptors.[8]

A bidentate ligand precursor containing accessible phosphine groups is an ideal precursor for post-synthetic modification. The ligand 6,6'-diphenylphosphino-2,2'-bipyridine $(Ph_2P)_2bpy$ contains four ligand donor groups that cannot simultaneously coordinate to a single metal, leaving PR_3 units poised for subsequent Staudinger reactions. Using this template (Figure 1), we targeted the incorporation of iminophosphorane moieties (derived from $(Ph_2P)_2bpy$) to generate a tetradentate ligand (two pyridine and two iminophosphorane units) capable of occupying the basal or equitorial plane in square pyramidal or octahedral complexes, respectively.

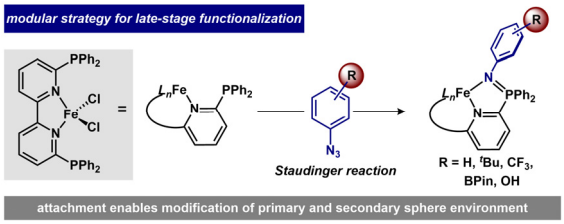

Figure 1. Conceptual design strategy for late-stage modification via the Staudinger reaction.

Our group is working to evaluate how the precise structural, electronic, and cooperative modes in the secondary coordination sphere can be used to regulate reactivity.[2g, 10] Although these secondary-sphere groups are often incorporated at an early stage, we are developing broadly adaptable synthetic strategies for both Brønsted and Lewis acid addition. Herein, we report the preparation of a 6,6-bis(diphenylphosphanyl)-2,2'-

[a] Department of Chemistry, University of Michigan, Ann Arbor, Michigan 48109, United States
[b] Department of Chemistry, The University of Jordan, Amman 11942, Jordan.
[c] H.C. Brown Laboratory, Department of Chemistry, Purdue University, West Lafayette, Indiana 47907, United States
† Electronic supplementary information (ESI) available. CCDC 2070170-2070174

bipyridyl iron(II) complex, a versatile late-stage modification platform, and demonstrate subsequent functionalization reactions.

Addition of $FeCl_2$ to 6,6-bis(diphenylphosphanyl)-2,2'-bipyridyl ($(Ph_2P)_2bpy$) in THF afforded an orange complex $(Ph_2P)_2bpyFeCl_2$ (**1**) in 84% yield after 18 h (Figure 2). The ^1H NMR spectrum in CD_2Cl_2 exhibits 6 sets of paramagnetically shifted signals from +75 to −16 ppm (μ_{eff} = 5.57, $CDCl_3$). A crystal of **1** suitable for X-ray diffraction was grown by vapor diffusion of diethyl ether into a concentrated dichloromethane-THF solution of **1** at room temperature (Fig. 2). This compound crystallizes in the space group *I*2, with two symmetry-independent molecules (see ESI). The crystal structure reveals a tetrahedral Fe(II) center (τ_4 = 0.87)[11] coordinated to the $(Ph_2P)_2bpy$ ligand. The metrical parameters of the Fe-ligand bond lengths in complex **1** are consistent with previously reported $Fe(bpy)Cl_2$ complexes (Fe(1)-N(1) = 2.125 (3) Å and (Fe(2)-N(2) = 2.121 (3) Å ; Fe(1)-Cl(1) = 2.2504(8) Å and Fe(2)-Cl(2) =2.2461(8) Å).[12] The Fe-P distances range from 3.301 to 3.297 Å, which is longer than the sum of the covalent radii, but within the sum of the Van der Waal radii.[13] Several intermolecular interactions (non-classical C-H···Cl, and C-H···C) connect the molecular units of **1** to form a two-dimensional array.

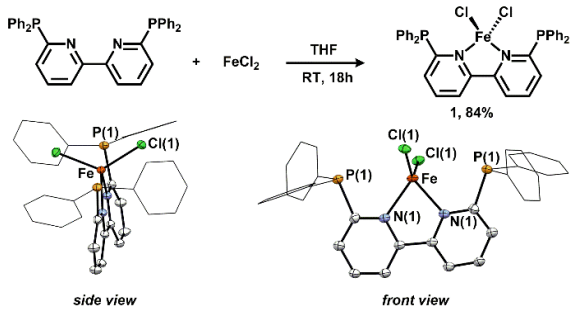

Figure 2. Synthesis and molecular structures (ORTEP, 50 % probability level) of **1**. Hydrogen atoms have been omitted and phenyl groups on phosphorus depicted in wireframe for clarity. Note that this corresponds to one of two symmetry independent molecules from the unit cell. Selected bond distances (Å): N(1)–Fe(1) = 2.125(3), Cl(1)–Fe(1) = 2.2504(8). Selected bond angles (°): Cl(1)–Fe(1)–Cl(1)= 125.12(6), N(1)–Fe(1)–N(1)= 77.34(16).

The structural analysis revealed the presence of appended phosphine groups available for subsequent functionalization via a Staudinger reaction. Treating an orange THF suspension of **1** with 2 equiv. of phenyl azide in the presence of 1 equiv. $NaPF_6$ afforded a color change to blue-green.[14] The resulting product, $\mathbf{2^H}$, was isolated as a microcrystalline solid in 95% yield. Analysis of the UV-Vis spectrum revealed a new feature at 615 nm (ε = 1791 M^{-1} cm^{-1}) and at 466 nm (ε = 1753 M^{-1} cm^{-1}). The MALDI mass spectrum of $\mathbf{2^H}$ showed incorporation of two N-Ph units (M-PF_6, m/z = 797.577), combustion analysis revealed an empirical formula of $C_{46}H_{36}ClF_6FeN_4P_3$, and the solution magnetic moment was consistent with an *S*=1 complex (μ_{eff} = 2.25; $CDCl_3$). These data support the formation of a new complex with incorporation of a new phenyl-iminophosphorane unit. Reactions using *para*-substituted aryl azides (*p*-CF_3, *p*-^{t}Bu) in place of Ph-N_3 afforded products $\mathbf{2^X}$ (X = CF_3, ^{t}Bu) that exhibited analogous characterization profiles (see ESI).

Crystallization of $\mathbf{2^H}$ from acetonitrile and diethyl ether afforded blue-green crystals suitable for X-ray diffraction. The

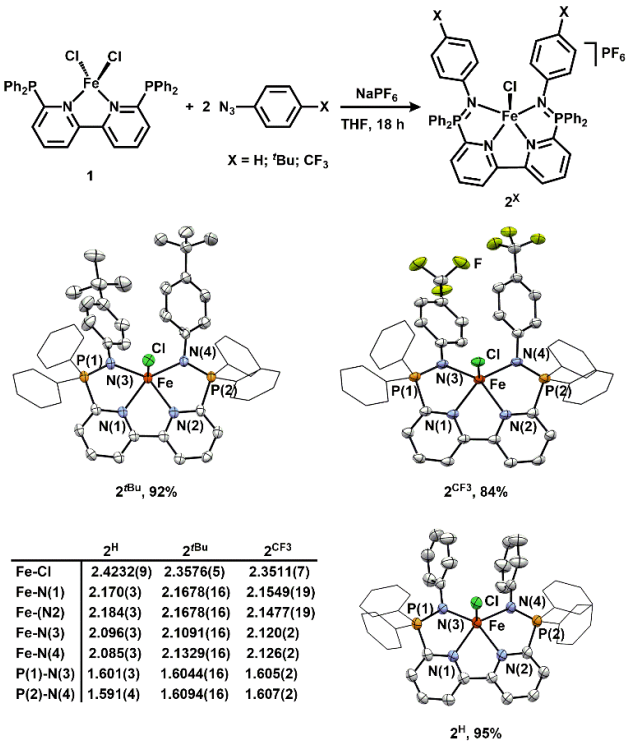

	2^H	2^{tBu}	2^{CF3}
Fe-Cl	2.4232(9)	2.3576(5)	2.3511(7)
Fe-N(1)	2.170(3)	2.1678(16)	2.1549(19)
Fe-(N2)	2.184(3)	2.1678(16)	2.1477(19)
Fe-N(3)	2.096(3)	2.1091(16)	2.120(2)
Fe-N(4)	2.085(3)	2.1329(16)	2.126(2)
P(1)-N(3)	1.601(3)	1.6044(16)	1.605(2)
P(2)-N(4)	1.591(4)	1.6094(16)	1.607(2)

Figure 3. Synthesis of $\mathbf{2^X}$. (i) Treatment 1 with two equiv. aryl azide and one equiv. $NaPF_6$, THF, RT, 18 h. Yields are based on 1. Ellipsoids depicted at 50 % probability. Hydrogen atoms have been omitted and phenyl groups on phosphorus depicted in wireframe for clarity.

molecular structure of $\mathbf{2^H}$ is shown in Figure 3. Distinct from **1**, the solid-state structure of $\mathbf{2^H}$ is best described as square based pyramidal (τ_5 < 0.05)[15] and the basal plane is occupied by the newly formed iminophosphorane units in addition to the two pyridine nitrogens. The unit cell contains three molecules, with two coordination environments: square pyramidal, with the fifth ligand being the halide, and octahedral, where the sixth ligand is occupied by MeCN solvent (Fig. S47, Fe–$NCCH_3$ = 2.285(3) Å). Compared to **1**, the Fe–pyridine bond lengths in $\mathbf{2^H}$ elongate (2.170(3) and 2.184(3) for Fe-N(1), and Fe-N(2), respectively) and have similar distances to the newly formed Fe-iminophosphorane bonds (2.096(3) and 2.178(3) for Fe-N(3) and Fe-N(4), respectively). The structures of $\mathbf{2^{tBu}}$ and $\mathbf{2^{CF3}}$ are square pyramidal (Fig. 3), with minimal differences to the primary coordination metrics. These data are consistent with distinct ligand donor properties in **1** and $\mathbf{2^X}$.

The electronic influence of each ligand variant was interrogated by cyclic voltammetry (Figure 4). Complex **1** exhibits a quasi-reversible Fe(II/III) redox couple (E_{pa} = 442 mV, E_{pc} = 303 mV; $E_{1/2}$ = 373 mV) vs Fc (CH_2Cl_2; 0.1 M $TBAPF_6$). The distinct primary coordination environment in complex $\mathbf{2^H}$ affords a reversible Fe(II/III) redox couple at 30 mV, and is shifted by ~350 mV more negatively than **1**. Across the series of para-substituted arenes, the redox potential underwent minimal additional tuning, with complex $\mathbf{2^{tBu}}$ at 184 mV and $\mathbf{2^{CF3}}$ at 160 mV (Figure 4). Although $\mathbf{2^H}$ and $\mathbf{2^{CF3}}$/$\mathbf{2^{tBu}}$ are shifted by

~150 mV, we ascribe the larger shift observed for $\mathbf{2^{H}}$ to MeCN coordination in the crystalline solid (see ESI). To better establish a difference in the electronic effect imparted by the new aryl groups, we turned to electronic absorption spectroscopy.

When dissolved in dichloromethane solvent, complexes $\mathbf{2^{X}}$ (X = CF_3, H, ^{t}Bu) exhibit two absorptions in the visible range. All three exhibit broad bands near ~600 nm and ~470 nm ($\mathbf{2^{CF3}}$: 593, 454 nm; $\mathbf{2^{H}}$: 615, 466 nm; $\mathbf{2^{tBu}}$: 630, 478 nm) with

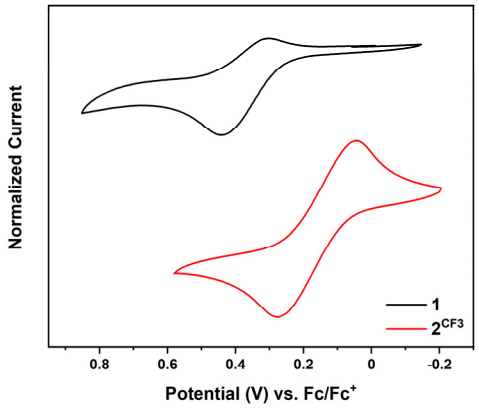

Figure 4. Cyclic voltammograms of **1** and $\mathbf{2^{CF3}}$: 0.1 M $[Bu_4N][PF_6]$, CH_2Cl_2, 100 mV/s.

extinction coefficients between 1000-3500 $M^{-1}cm^{-1}$, consistent with metal to ligand charge transfer transitions.[16] These bands are sensitive to the para-substituent of the newly installed *N*-bound arene; we obtained linear correlations between the Hammett σ_p values[17] and the energies of the absorbance bands (R^2 > 0.94). Complex $\mathbf{2^{CF3}}$ has the highest energy transitions (16900, 22000 cm^{-1}) followed by $\mathbf{2^{H}}$ (16300, 21500 cm^{-1}) and $\mathbf{2^{tBu}}$ (15900, 20900 cm^{-1}). These data indicate a systematic shift to higher energy as the para-substituent becomes more electron withdrawing.[18]

After establishing the Staudinger reaction as a robust strategy to install aryl groups on **1**, we targeted variants of **2** that contain either Brønsted or Lewis acidic pendent groups. Brønsted-acidic appended groups were incorporated by allowing either 2- or 3-OH-phenyl azide to react with **1** to afford $\mathbf{2^{2\text{-}OH}}$ and $\mathbf{2^{3\text{-}OH}}$ in 90% and 75% yield, respectively. Although $\mathbf{2^{3\text{-}OH}}$ exhibits similar spectroscopic features to the rest of series of $\mathbf{2^{X}}$ (λ_{max} = 606 nm; ε = 2273 M^{-1} cm^{-1}), $E_{1/2}$ = 25 mV). However, $\mathbf{2^{2\text{-}OH}}$ displayed distinct features in the UV-vis spectrum (690 nm), voltammetry ($E_{1/2}$ = –465 mV), as well as the MALDI-TOF MS (792.405 m/z = $\mathbf{2^{2\text{-}OH}}$-HCl- PF_6^-). These results are consistent with a primary sphere containing Fe-OPh coordination, rather than Fe-Cl, formed *via* deprotonation of the appended –OH groups. Boron Lewis acids were installed using Bpin-functionalized phenyl azides. Although weakly Lewis acidic, BPin units have been shown to interact with metal-coordinated substrates when spatially predisposed.[19] Lewis acid appended groups were incorporated by allowing either 2-BPin or 3-BPin-phenyl azide to react with **1**. The products, $\mathbf{2^{2\text{-}BPin}}$ and $\mathbf{2^{3\text{-}Bpin}}$ exhibited similar spectroscopic characteristics as the series of $\mathbf{2^{x}}$ ($\mathbf{2^{2\text{-}BPin}}$: λ_{max} = 596 nm; ε = 1127 M^{-1} cm^{-1}, λ_{max} = 439 nm; ε = 1615 M^{-1} cm^{-1}, $E_{1/2}$ = 178 mV; $\mathbf{2^{3\text{-}BPin}}$: λ_{max} = 628 nm; ε = 1255 M^{-1} cm^{-1}, λ_{max} = 474 nm; ε = 1127 M^{-1} cm^{-1}, $E_{1/2}$ = 239 mV) consistent with an isostructural primary coordination sphere.

Vapour diffusion of diethyl ether into acetonitrile solution of $\mathbf{2^{3\text{-}BPin}}$ afford blue-green crystals amenable to an X-ray diffraction experiment. The molecular structure of $\mathbf{2^{3\text{-}BPin}}$ (Fig. 5) is commensurable to the series of $\mathbf{2^{X}}$, with similar Fe-ligand

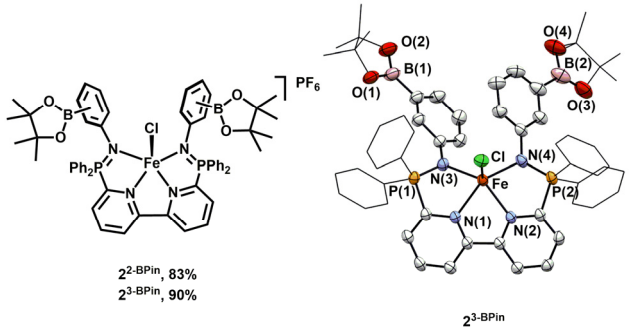

Figure 5. Structures of $\mathbf{2^{2\text{-}BPin}}$ and $\mathbf{2^{3\text{-}BPin}}$. Molecular structure (ORTEP, 50 % probability level) of $\mathbf{2^{3\text{-}BPin}}$. Hydrogen atoms, BPin and phenyl groups on phosphorus depicted in wireframe for clarity, and counter ion omitted. Selected bond distances (Å): N(1)–Fe(1) = 2.152(2), N(2)–Fe(1) = 2.152(2), N(3)–P(1) = 1.604(2), N(3)–Fe(1) = 2.102(2), N(4)–P(2) = 1.604(2), N(4)–Fe(1) = 2.105(2), Cl(1)–Fe(1) = 2.3723(8).

bond lengths and geometry around the Fe(II) center (τ_5 = 0.111). The boron atoms in the BPin unit are planar (Σ > 359°), consistent with an unquenched Lewis acid. Although the BPin units appear unquenched in $\mathbf{2^{3\text{-}BPin}}$ and $\mathbf{2^{2\text{-}BPin}}$, we anticipate that they may engage in Lewis acid/base interactions with an appropriate Lewis basic substrate. Overall, the preparation of $\mathbf{2^{X}}$ containing appended –OH and –Bpin units establishes the viability of this late-stage functionalization approach.

In conclusion, we report that **1**, a tetrahedral iron complex with appended diphenylphosphine units is amenable to late-stage functionalization via Staudinger reactions. Addition of aryl azides afforded a series of five-coordinate Fe(II) iminophosphorane compounds, $\mathbf{2^{X}}$. These modified complexes exhibit distinct ligand electronic and steric properties, and importantly the electronic properties are tunable as a function of para-substitution. This ligand modification methodology enabled late-stage functionalization with both Brønsted and Lewis acids, and we anticipate these or related complexes may ultimately be exploited as metal ligand cooperative platforms.

ACKNOWLEDGMENT

This work was supported by the NSF (CHE-1900257; N.K.S) and The University of Jordan and the Arab Fund (D.T). N.K.S. is a Camille Dreyfus Teacher-Scholar. X-ray diffractometers were funded by the NSF under Award CHE 1625543 (M.Z.).

Conflicts of interest

The authors declare no competing financial interests.

Notes and references

1. *Bifunctional Molecular Catalysis*, Springer-Verlag Berlin Heidelberg, 1 edn., 2011.
2. (a) A. Maity and T. S. Teets, *Chem. Rev.*, 2016, **116**, 8873-8911; (b) W. Guan, G. Zeng, H. Kameo, Y. Nakao and S. Sakaki, *Chem. Rec.*, 2016, **16**, 2405-2425; (c) Y. Gao, C. Guan, M. Zhou, A. Kumar, T. J. Emge, A. M. Wright, K. I. Goldberg, K. Krogh-Jespersen and A. S. Goldman, *J. Am. Chem. Soc.*, 2017, **139**, 6338-6350; (d) A. L. Liberman-Martin, D. S. Levine, W. Liu, R. G. Bergman and T. D. Tilley, *Organometallics*, 2016, **35**, 1064-1069; (e) A. L. Liberman-Martin, R. G. Bergman and T. D. Tilley, *J. Am. Chem. Soc.*, 2013, **135**, 9612-9615; (f) K.-N. T. Tseng, J. W. Kampf and N. K. Szymczak, *ACS Catal.*, 2015, **5**, 411-415; (g) L. V. A. Hale and N. K. Szymczak, *ACS Catalysis*, 2018, **8**, 6446-6461; (h) C. Brennan, A. Draksharapu, W. R. Browne, J. J. McGarvey, J. G. Vos and M. T. Pryce, *Dalton Trans.*, 2013, **42**, 2546-2555; (i) S. Fanni, S. Murphy, J. S. Killeen and J. G. Vos, *Inorg. Chem.*, 2000, **39**, 1320-1321; (j) O. Costisor and W. Linert, *Metal Mediated Template Synthesis of Ligands*, WORLD SCIENTIFIC, 2004; (k) J. R. Khusnutdinova and D. Milstein, *Angew. Chem. Int. Ed.*, 2015, **54**, 12236-12273.
3. (a) J. J. Kiernicki, M. Zeller and N. K. Szymczak, *Inorg. Chem.*, 2019, **58**, 1147-1154; (b) K.-N. T. Tseng, J. W. Kampf and N. K. Szymczak, *J. Am. Chem. Soc.*, 2016, **138**, 10378-10381. (c) K.-N. T. Tseng, J. W. Kampf and N. K. Szymczak, *J. Am. Chem. Soc.*, 2017, **139**, 18122-18122
4. F. Palacios, C. Alonso, D. Aparicio, G. Rubiales and J. M. de los Santos, *Tetrahedron*, 2007, **63**, 523-575.
5. (a) S. Rothemund and I. Teasdale, *Chem. Soc. Rev.*, 2016, **45**, 5200-5215; (b) H. Krawczyk, M. Dzięgielewski, D. Deredas, A. Albrecht and Ł. Albrecht, *Chem. Eur. J.*, 2015, **21**, 10268-10277.
6. (a) S. Ge, J. Zhao, M. J. Ferguson, G. Ma and R. G. Cavell, *Organometallics*, 2020, **39**, 478-486; (b) B. Murugesapandian, M. Kuzdrowska, M. T. Gamer, L. Hartenstein and P. W. Roesky, *Organometallics*, 2013, **32**, 1500-1506; (c) P. Molina, A. Arques, A. García and M. C. Ramírez de Arellano, *Eur. J. Inorg. Chem.*, 1998, **1998**, 1359-1368.
7. A post-metalation route has been reported, which may involve metal-mediated imidation of a coordinated phosphine. (a) J. Xiao and L. Deng, *Dalton Trans*., 2013, 42, 5607-5610; (b) M. J. Ingleson, M. Pink, H. Fan and K. G. Caulton, J. Am. Chem. Soc., 2008, 130, 4262-4276; (c) W. A. Chomitz and J. Arnold, Inorg. Chem., 2009, 48, 3274-3286; (d) X. Hu and K. Meyer, J. Am. Chem. Soc., 2004, 126, 16322-16323.
8. (a) R. Bielsa, R. Navarro, T. Soler and E. P. Urriolabeitia, *Dalton Trans.*, 2008, 1203-1214; (b) D. Aguilar, R. Bielsa, M. Contel, A. Lledós, R. Navarro, T. Soler and E. P. Urriolabeitia, *Organometallics*, 2008, **27**, 2929-2936; (c) D. Aguilar, R. Navarro, T. Soler and E. P. Urriolabeitia, *Dalton Trans.*, 2010, **39**, 10422-10431; (d) D. Aguilar, G. González, P. Villuendas and E. P. Urriolabeitia, *J. Organomet. Chem.*, 2014, **767**, 27-34; (e) J. Vicente, J.-A. Abad, R. Clemente, J. López-Serrano, M. C. Ramírez de Arellano, P. G. Jones and D. Bautista, *Organometallics*, 2003, **22**, 4248-4259.
9. R. Ziessel, *Tetrahedron Lett.*, 1989, **30**, 463-466.
10. (a) E. W. Dahl, H. T. Dong and N. K. Szymczak, *Chem. Commun.*, 2018, **54**, 892-895; (b) E. W. Dahl, J. J. Kiernicki, M. Zeller and N. K. Szymczak, *J. Am. Chem. Soc.*, 2018, **140**, 10075-10079; (c) J. P. Shanahan and N. K. Szymczak, *J. Am. Chem. Soc.*, 2019, **141**, 8550-8556; (d) E. W. Dahl and N. K. Szymczak, *Angew. Chem. Int. Ed.*, 2016, **55**, 3101-3105.
11. A. Okuniewski, D. Rosiak, J. Chojnacki and B. Becker, *Polyhedron*, 2015, **90**, 47-57.
12. (a) B. C. K. Chan and M. C. Baird, *Inorg. Chim. Acta*, 2004, **357**, 2776-2782; (b) Y. Matsubara, T. Yamaguchi, T. Hashimoto and Y. Yamaguchi, *Polyhedron*, 2017, **128**, 198-202.
13. (a) B. Cordero, V. Gómez, A. E. Platero-Prats, M. Revés, J. Echeverría, E. Cremades, F. Barragán and S. Alvarez, *Dalton Trans.*, 2008, 2832-2838; (b) S. S. Batsanov, *Inorg. Mater.*, 2001, **37**, 871-885.
14. Mixtures of products, rather than clean conversion to a single product was observed in the absence of $NaPF_6$.
15. A. W. Addison, T. N. Rao, J. Reedijk, J. van Rijn and G. C. Verschoor, *J. Chem. Soc., Dalton Trans.*, 1984, 1349-1356.
16. (a) D. Mandon, A. Machkour, S. Goetz and R. Welter, *Inorg. Chem.*, 2002, **41**, 5364-5372; (b) M. Narwane, Y.-L. Chang, W.-M. Ching, M.-L. Tsai and S. C. N. Hsu, *Inorg. Chim. Acta*, 2019, **495**, 118966; (c) G. J. P. Britovsek, V. C. Gibson, S. K. Spitzmesser, K. P. Tellmann, A. J. P. White and D. J. Williams, *J. Chem. Soc., Dalton Trans.*, 2002, 1159-1171.
17. C. Hansch, A. Leo and R. W. Taft, *Chem. Rev.*, 1991, **91**, 165-195.
18. S. Ganguly, L. J. Giles, K. E. Thomas, R. Sarangi and A. Ghosh, *Chem. Eur. J.*, 2017, **23**, 15098-15106.
19. O. Tutusaus, C. Ni and N. K. Szymczak, *J. Am. Chem. Soc.*, 2013, **135**, 3403-3406.

